A Closed-Form Full-Wave Model for the Reflection Coefficient of an Open-Ended Coaxial Probe for Real-Time Dielectric Spectroscopy

Hossein Asilian Bidgoli
Systems and Computer Engineering
Carleton University
Ottawa, Canada
hosseinasilianbidgo@cmail.carleton.ca

Nicola Schieda
Radio., Rad. Oncology and Med. Physics
University of Ottawa
Ottawa, Canada
nschieda@toh.ca

Carlos Rossa
Systems and Computer Engineering
Carleton University
Ottawa, Canada
rossa@sce.carleton.ca

***Abstract*—Dielectric spectroscopy using open-ended coaxial probes characterizes the permittivity of a material based on its interference with a transmitted electromagnetic wave, offering many applications spanning from human health to non-destructive testing. The permittivity is uniquely tied to the material's reflection coefficient, that is, the ratio between the magnitude of the reflect wave to that of the incident wave. Various models have been proposed to relate the permittivity of the material to the measured reflection coefficient, but they all suffer from a common trade off: When they favour simplicity, they neglect higher order modes and become inaccurate. When using full-wave analysis, they are indeterminate, computationally intensive with no closed-form solution, and cannot be used in real-time.**

In this paper we introduce for the first time a novel full-wave, closed-form model for the reflection coefficient of an open-ended coaxial probe. Our novel model combines full-wave analysis with a Taylor series expansion to reduced the forward problem to a simple matrix inversion, significantly reducing the computational costs of full-wave analysis, while maintaining unparalleled accuracy. The proposed model is validated experimentally through 200 measurements in methanol and with extended permittivity ranges over 1800 simulations in Ansys. The average modelling errors compared to experimental and simulation results are 0.92% and 1.5%, respectively, making this model a significant step towards full-wave real-time spectroscopy.

***Index Terms*—Dielectric spectroscopy; reflection coefficient; closed-form model; open-ended coaxial probe; full-wave model.**

I. Introduction

Permittivity spectroscopy via open-ended coaxial probes is an instrumentation technique that determines the complex permittivity of a medium over a wide frequency band. The concept involves passing a transverse electromagnetic (TEM) wave through the probe to observe how the material under test (MUT) perturbs the electromagnetic field. Due to the impedance discontinuity at the aperture of the probe, part of the incident wave is reflected back to the source. The ratio of the complex amplitude of the reflected wave to that of the incident wave, called the reflection coefficient, is uniquely tied to the MUT's dielectric properties.

Accurate permittivity estimation from measurements of the reflected wave relies on a model that can unambiguously describe the electromagnetic field at the aperture of the coaxial probe and infer what the properties of the MUT must have been to perturb the incident wave and generate the reflected wave observed back at the source. Given a particular probe's geometry, only certain patterns of electromagnetic field, called modes, can exist for waves propagating inside the probe. These modes are the solutions to the governing partial differential wave equations derived from Maxwell's equations. The weighted sum of these modes must satisfy the boundary conditions that ensure continuity of the field near the aperture of the probe.

The simplest and arguably most prominent approach to determine the reflection coefficient of the TEM wave (the primary reflection coefficient) models the MUT as an equivalent lumped circuit consisting of a resistance and a capacitance in parallel placed at the end of the probe [1]–[6]. The capacitance and resistance of the circuit are functions of the complex permittivity of the MUT. While simple and computationally efficient, these models are only valid under strict conditions, such as narrow frequency and permittivity ranges, and in consequence have limited usefulness [7].

A more rigorous modelling approach considers how the TEM wave propagates inside the probe as the basis to derive an admittance model of the aperture in contact with the MUT [8]–[12]. The underlining principle equates the electromagnetic and radiated fields within the probe and assumes the electric field at any point in the cross section of the line to be proportional to the radial distance from its longitudinal axis. An inherent limitation of this approach is that a closed-form solution for the primary reflection coefficient does not exist since the model requires solving for multi-variable integrations that are simultaneously dependent on the geometry of the probe and the MUT parameters. This makes the normalized admittance model computationally expensive and unsuitable for real-time applications [13], [14].

This research is supported by the Canadian Cancer Society and the Canadian Institutes of Health Research (grant #944486). Cette recherche est appuyée par la Société canadienne du cancer et les instituts de recherche en santé du Canada (subvention no 944486).

Approximate closed-form models of the reflection coefficient involving the primary mode use Taylor expansion to free these integrals from the MUT's properties, allowing for faster computation compared to the corresponding analytical solution [15], [16]. The Taylor expansion leads to a weighted sum of the MUT wave number raised to the power of an increasing integer. The weight of each parameter in the expansion can be calculated analytically or found through model fitting [17], [18]. All these model share the same major limitation: By treating only the TEM, higher-order modes generated at the aperture are ignored, making them unsuitable in frequencies where the field wavelength approaches the size of the aperture and the effect of high order modes cannot be neglected [19]. Indeed, the reflected wave is a combination of the incident TEM and higher order transverse magnetic (TM) modes arising from field perturbations. Unlike the TEM, these higher order TM modes are evanescent, i.e., they do do not propagate back to the source and hence cannot be measured directly. A model of the primary reflection coefficient for the purpose of estimating the permittivity of the MUT must, therefore, include all wave modes.

Expanding on primary mode models, full-wave methods that account for higher order TM modes have also been proposed. The reflection coefficient is determined by subjecting the resulting wave equation to boundary conditions at the probe's aperture that ensure continuity of the electromagnetic field, that is, the radiated wave and the TEM and TM waves inside the coaxial cable must be the same [20], [21]. However, these methods rely on lengthy mathematical manipulations with multiple integrals over the properties of both the MUT and geometric characteristics of the probe, simultaneously, while being subjected to local singularities. Similar to primary mode approaches, these models are indeterminate and no closed-form solution has been found, requiring the use of an inverse problem to infer the reflection coefficient given the permittivity of the MUT. While solving for these integrals numerically is feasible, the process is computationally heavy, much more time intensive than analytical admittance models, and cannot be used in real-time. Despite over half a century of continuous incremental development, a full-wave, closed-form solution for the reflection coefficient of an open-ended coaxial problem still remains a critical open challenge in dielectric spectroscopy.

In this paper we introduce for the first time a full-wave and closed-form model for the reflection coefficient of an open-ended coaxial probe. Our model addresses a crucial gap in the current state-of-the-art and is expected to eliminate the well-known inaccuracies and limitations of single mode models, while significantly reducing the computational costs required in full-wave analysis. Our principle expands on past work by combining a full-wave model with a Taylor series expansion that reduces the forward problem to a simple matrix inversion. Dielectric spectroscopy primarily serves to determine material permittivity. This is achieved through the solution of an inverse problem using methods such as Newton-Raphson. Implementing the proposed model in this context would substantially accelerate computation time for solving inverse problems.

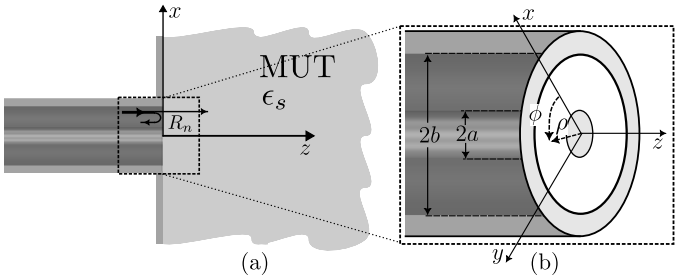

Fig. 1. (a) Open-ended coaxial probe in contact with a MUT of permittivity ϵ_s. The reflection coefficients is denoted by R_n. (b) The coaxial probe aperture in cylindrical coordinates ρ and ϕ, with reference frame xyz at the centre of the aperture. a and b are the inner and outer radii of the probe.

The model is validated experimentally through 200 measurements in methanol with a frequency ranging from 0.5 GHz to 5 GHz, and further validated with extended permittivity ranges over 1800 simulations in *Ansys*. The experimental and simulation results show an average modelling error of 1.5% and 0.92%, respectively. This model is a crucial first step towards implementing full-wave, real-time dielectric spectroscopy, which has many applications in human health.

The paper is structured as follows: Section II presents the formulation procedure leading to the proposed model. Section IV validates the model through experimental results and simulation, followed by a conclusion in Section V.

II. Wave Propagation and Radiation in a Coaxial Probe

We begin by laying out the well-known equations describing the propagation of both the electric and magnetic fields inside the coaxial probe, as well as the magnetic wave radiated to the MUT from the aperture.

The electromagnetic field inside the probe is the solution to the Helmholtz equation. The TEM wave has an electric and a magnetic field perpendicular to the direction of propagation, while TM waves have perpendicular magnetic and electric components in addition to a parallel electric field. The incident wave consists solely of the TEM wave, while the reflected wave is a summation of the TEM and the TM waves [9], [22]. Assuming the probe is oriented with its longitudinal axis along the z-axis (direction of wave propagation), as in Fig. 1, the radial electric field E_ρ can be expressed as follows:

$$E_\rho(\rho, z) = A_0 \left[f_0(\rho) \mathrm{e}^{-\gamma_0 z} + \sum_{n=0}^{\infty} R_n f_n(\rho) \mathrm{e}^{\gamma_n z} \right] \quad (1)$$

And the azimuthal magnetic field H_ϕ is:

$$H_\phi(\rho, z) = j\omega\epsilon_0\epsilon_c A_0 \left[\frac{f_0(\rho)}{\gamma_0} \mathrm{e}^{-\gamma_0 z} - \sum_{n=0}^{\infty} R_n \frac{f_n(\rho)}{\gamma_n} \mathrm{e}^{\gamma_n z} \right] \quad (2)$$

where A_0 is the amplitude of the primary mode of the electric field, $f_n(\rho)$ is the radial function of each mode n as given in [21], in which ρ is the azimuth angle of the aperture (see Fig. 1), and γ_n is the propagation factor of mode n. The

reflection coefficient of each mode is R_n. Of particular interest is the primary reflection mode R_0 (for $n = 0$), which is the only measurable parameter of the reflected wave. Other parameters are as follows: ϵ_0 is the vacuum permittivity, ϵ_c is the relative permittivity of dielectric inside the probe, ω is the radial frequency, and k_s is the MUT wave number. The MUT wave number is a function of its complex permittivity ϵ_s^*:

$$k_s = \omega\sqrt{\mu_0\epsilon_0\epsilon_s^*}, \tag{3}$$

and the MUT complex relative permittivity is:

$$\epsilon_s^* = \epsilon_s - j\frac{\sigma_s}{\omega\epsilon_0}, \tag{4}$$

where ϵ_s and σ_s are the relative permittivity and conductivity of the MUT, respectively.

The radiated magnetic field relates to the tangential electric at the aperture via Huygens's principle as follows [9]:

$$H_\phi(\rho, z) = \frac{jk_s^2}{2\pi\omega\mu_0}\int_a^b E_\rho(\rho')\,\rho'\mathrm{d}\rho'\int_0^{2\pi}\frac{e^{-jk_s r}}{r}\cos\psi\mathrm{d}\psi\mathrm{d}\rho' \tag{5}$$

The boundary conditions must ensure that the magnetic field inside and outside the probe are equal at the aperture. This condition is satisfied by equating (2) and (5) at $z = 0$:

$$\begin{aligned} &j\omega\epsilon_0\epsilon_c A_0\left[\frac{f_0(\rho)}{\gamma_0} - \sum_{n=0}^{\infty} R_n\frac{f_n(\rho)}{\gamma_n}\right] = \\ &\frac{jk_s^2}{2\pi\omega\mu_0}\int_a^b\int_0^{2\pi} E_\rho(\rho')\frac{e^{-jk_s r}}{r}\cos\psi\rho'\mathrm{d}\psi\mathrm{d}\rho' \end{aligned} \tag{6}$$

A common approach used for calculating the normalized admittance of the coaxial probe is to replace the electric field with its TEM mode, i.e., $E(\rho) = E_0/\rho$ [15], [23]. However, this method sacrifices accuracy by neglecting higher-order modes in favour of simplicity. Also, from the normalized admittance model, a closed-form model can be achieved by replacing the exponential function $e^{-jk_s r}$ with a Taylor expansion, thereby making the integral independent of the material properties and solely reliant on the probe geometry and its dielectric permittivity [16], [17]. Although this method is simple and rather efficient, it tends to fail when the aperture diameter is close to operating frequency wavelength. To address this limitation, the coefficients of the Taylor expansion may be optimized through analytical calculations [18], or by model fitting [17]. However, significant modelling errors still remain since higher modes are not taken into account.

III. Proposed Full-Wave Model in Closed-Form

In the proposed full-wave model the electric field $E_\rho(\rho')$ in (6) is replaced with its full-wave form from (1). Thus, (6) can be rewritten as:

$$\begin{aligned} &j\omega\epsilon_0\epsilon_c A_0\left[\frac{f_0(\rho)}{\gamma_0} - \sum_{n=0}^{\infty} R_n\frac{f_n(\rho)}{\gamma_n}\right] = \frac{jk_s^2}{2\pi\omega\mu_0}\int_a^b\int_0^{2\pi} \\ &A_0\left[f_0(\rho') + \sum_{n=0}^{\infty} R_n f_n(\rho')\right]\frac{e^{-jk_s r}}{r}\cos\psi\rho'\mathrm{d}\psi\mathrm{d}\rho' \end{aligned} \tag{7}$$

Up to this point, the approach we have taken is that of full-wave analytical models [20], [21]. The unknown parameter in this equation is the reflection coefficient R_n. Various methods have been employed to create a system of equations from (7) to solve for R_n. These methods involve several numerical integrals and the process is computationally intensive, the integrals are subjected to singularities, and they must be computed for every single measurement point. Even more time consuming is the process of determining the permittivity of the MUT through a resulting iterative inverse problem over the forward model, making real-time measurements impossible.

To circumvent the need for numerically evaluating the reflection coefficient model for each measurement, we note that the only variable in (7) that entangles the MUT properties is $e^{-jk_s r}$ on the right hand side of the equation. All the remaining terms are either the known TEM or TM wave modes, or the geometric and dielectric parameters of the probe. To solve for R_n in (7), we begin by replacing the exponential term with a corresponding Taylor series expansion, similarly to TEM-only models [12], [15], [16]:

$$\frac{e^{-jk_s r}}{r} = \sum_{p=0}^{\infty}\frac{(-jk_s)^p r^{p-1}}{p!} \tag{8}$$

This manipulation will lead to several integrals that are solely a function of the probe geometry. The MUT properties are then multiplied by the result of these integrals. It follows that after the expansion (7) changes to

$$\begin{aligned} &j\omega\epsilon_0\epsilon_c A_0\left[\frac{f_0(\rho)}{\gamma_0} - \sum_{n=0}^{\infty} R_n\frac{f_n(\rho)}{\gamma_n}\right] = \frac{jk_s^2}{2\pi\omega\mu_0}\int_a^b\int_0^{2\pi} A_0 \\ &\left[f_0(\rho') + \sum_{n=0}^{\infty} R_n f_n(\rho')\right]\left[\sum_{p=0}^{\infty}\frac{(-jk_s)^p r^{p-1}}{p!}\right]\cos\psi\rho'\mathrm{d}\psi\mathrm{d}\rho' \end{aligned} \tag{9}$$

Both sides of the equality in (9) are functions of ρ. To establish a system of equations to solve for R_n and eliminate the dependency on ρ, we multiply both sides of (9) by $f_m(\rho)\rho$ and integrate over ρ from a to b. For mode $m = 0$, the above yields:

$$\begin{aligned} &\frac{\epsilon_c}{\epsilon_s\gamma_0}(1 - R_0)\int_a^b f_0^2(\rho)\rho\,\mathrm{d}\rho = \\ &\frac{1}{2\pi}\int_a^b\int_a^b\int_0^{2\pi}\left[(1 + R_0)f_0(\rho') + \sum_{n=1}^{\infty} R_n f_n(\rho')\right] \\ &\left[\sum_{p=0}^{\infty}\frac{(-jk_s)^p r^{p-1}}{p!}\right] f_0(\rho)\cos\psi\rho'\mathrm{d}\psi\,\mathrm{d}\rho'\,\mathrm{d}\rho \end{aligned} \tag{10}$$

And for $m > 0$, we have:

$$\begin{aligned} &\frac{\epsilon_c}{\epsilon_s\gamma_m}(-R_m)\int_a^b f_0^2(\rho)\rho\,\mathrm{d}\rho = \\ &\frac{1}{2\pi}\int_a^b\int_a^b\int_0^{2\pi}\left[(1 + R_0)f_0(\rho') + \sum_{n=1}^{\infty} R_n f_n(\rho')\right] \\ &\left[\sum_{p=0}^{\infty}\frac{(-jk_s)^p r^{p-1}}{p!}\right] f_m(\rho)\cos\psi\rho\rho'\mathrm{d}\psi\,\mathrm{d}\rho'\,\mathrm{d}\rho \end{aligned} \tag{11}$$

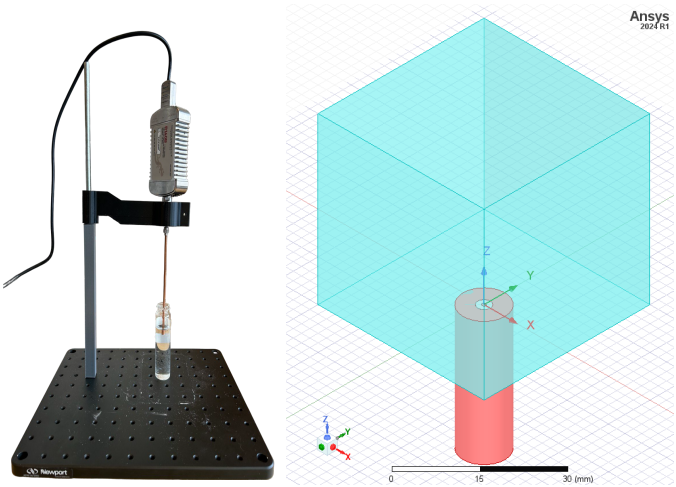

(a) (b)

Fig. 2. (a) Experimental setup used for model validation showing the vector network analyzer with a coaxial probe placed in methanol. (b) Full-wave simulation of an open-ended coaxial probe inside a MUT (blue cube) in Ansys.

The orthogonality of Bessel function states that:

$$\int_a^b f_n(\rho) f_m(\rho) \rho \mathrm{d}\rho = 0 \quad if \quad n \neq m \tag{12}$$

which entails that only one integral on the left side of (10) and (11) is not zero. Thus, these equations may be rewritten as a double summations, i.e., for $m = 0$:

$$(1 - R_0)\frac{\epsilon_c}{\epsilon_s \gamma_0}\alpha_0 = (1 + R_0)\sum_{p=0}^{\infty}(-jk_s)^p \beta_{00p} + \sum_{n=1}^{\infty} R_n \sum_{p=0}^{\infty}(-jk_s)^p \beta_{0np} \tag{13}$$

And for $m > 0$:

$$(-R_m)\frac{\epsilon_c}{\epsilon_s \gamma_m}\alpha_m = (1 + R_0)\sum_{p=0}^{\infty}(-jk_s)^p \beta_{m0p} + \sum_{n=1}^{\infty} R_n \sum_{p=0}^{\infty}(-jk_s)^p \beta_{mnp} \tag{14}$$

where the coefficient α_m can be calculated as follows:

$$\alpha_m = \int_a^b f_m^2(\rho) \rho \mathrm{d}\rho \tag{15}$$

And for β_{mnp} we have:

$$\beta_{mnp} = \frac{1}{2\pi}\int_a^b \int_a^b \int_0^{2\pi} \frac{r^{p-1}}{p!} f_n(\rho') f_m(\rho) \rho' \rho \cos\psi \mathrm{d}\psi \mathrm{d}\rho' \mathrm{d}\rho \tag{16}$$

These equations can be expressed as a simple matrix multiplication:

$$AR = B \tag{17}$$

where A and B are given in (17) and (18). In these matrices the sums are defined from $p = 0$ to $p \to \infty$, i.e., $\sum \to \sum_{p=0}^{\infty}$. These limits are omitted for simplicity. Finally, R_0 is simply found as the first cell of the vector $R = (A^{-1})B$.

It is important to highlight that all coefficients in A must be calculated only once for each probe, and unlike previously reported models, they are independent from the properties of the MUT. The proposed closed-form model involves a simple matrix operation, which is inherently fast, especially with modern CPUs and GPUs optimized for vector calculation.

IV. Model Validation

The proposed model will first be validated experimentally, and then through simulations with a wider range of MUT properties. We consider a standard 50 Ω coaxial cable with a relative permittivity of $\epsilon_c = 2.08$ and inner and outer radii of $a = 0.46$ mm and $b = 1.5$ mm, respectively. According to, [21]exceeding five modes does not notably enhance accuracy. This means that a total of 125 different β_{mnp} coefficients must be calculated in (16), and another 5 different α_m must be determined in (15). Python code has been written for matrix calculations, utilizing the scipy.linalg library, which is LAPACK-based, for matrix inversion of matrix A.

The experimental setup is depicted in Figure 2(a). One end of the probe is connected to a vector network analyzer (VNA) (model R140B from Copper Mountain) while the aperture is submerged in pure methanol. The calibration procedure outlined in [12] is used in this study, with water, ethanol, and air serving as reference materials. The permittivity of the MUT is known. The reflection coefficient is measured through the VNA between 1 GHz and 5 GHz with intervals of 20 MHz.

Experimental results: The complex and real part of the measured and model-estimated reflection coefficient are presented in a polar plot in Fig. 3. Notably, the model demonstrate strong agreement with the experimental data. The average relative error between the measurements and the model is found to be 0.92%.

To further validate the model with a wider range of MUT properties, simulations were conducted using Ansys HFSS Electromagnetic Simulator. Fig. 2(b) shows the simulation environment, where the blue cube is the MUT. Two sets of simulations were carried out to determine the reflection coefficient of the probe when in contact with the MUT:

1) Simulation 1: In the first set, the relative permittivity of the MUT is swept from $\epsilon_s = 1$ to $\epsilon_s = 100$, and the conductivity ranges from $\sigma_s = 0$ S/m to $\sigma_s = 5$ S/m, with steps of 5 and 0.1 S/m respectively. This process is repeated at 0.5 GHz, 1 GHz, and 5 GHz.
2) Simulation 2: In the second set, water, ethanol, and methanol are simulated as the MUT with a frequency ranging from 1 GHz to 5 GHz with steps of 20 MHz.

Simulation results: The simulation results are summarized in Figs. 4 and 5. In Fig. 4, every point on the polar plot stems from an unique combination of the MUT permittivity and conductivity, while the colour of each point gives the relative error between the model-predicted and the simulated complex

$$A = \begin{bmatrix} \sum(-jk_s)^p\beta_{00p} + \frac{\epsilon_c}{\epsilon_s\gamma_0}\alpha_0 & \sum(-jk_s)^p\beta_{01p} & \cdots & \sum(-jk_s)^p\beta_{0Np} \\ \sum(-jk_s)^p\beta_{10p} & \sum(-jk_s)^p\beta_{11p} + \frac{\epsilon_c}{\epsilon_s\gamma_1}\alpha_1 & \cdots & \sum(-jk_s)^p\beta_{1Np} \\ \vdots & \vdots & \ddots & \vdots \\ \sum(-jk_s)^p\beta_{N0p} & \sum(-jk_s)^p\beta_{N1p} & \cdots & \sum(-jk_s)^p\beta_{NNp} + \frac{\epsilon_c}{\epsilon_s\gamma_N}\alpha_N \end{bmatrix} \tag{17}$$

$$B = \begin{bmatrix} \frac{\epsilon_c}{\epsilon_s\gamma_0}\alpha_0 - \sum(-jk_s)^p\beta_{00p} & -\sum(-jk_s)^p\beta_{10p} & \cdots & -\sum(-jk_s)^p\beta_{N0p} \end{bmatrix}^T \tag{18}$$

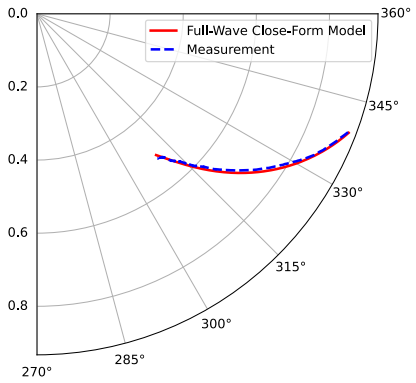

Fig. 3. Model-estimated vs measured reflection coefficient in methanol for a frequency range of 1 GHz to 5 GHz. The relative modelling error is 0.92%.

value of the reflection coefficient. The relative error can be defined as follows:

$$\text{Error} = \frac{1}{k}\sum_{i=1}^{k}\left|\frac{R_{sim,i} - R_{model,i}}{R_{sim,i}}\right| \tag{18}$$

where k is the number of points, and $R_{0,sim}$ and $R_{0,model}$ are the primary reflection coefficient from simulation and proposed model, respectively. For frequencies of 0.5 GHz and 1 GHz the maximum error is less than 1%. At 5 GHz the largest error is around 2.5%, happening when $\sigma_s = 5S/m$. Overall, the error increases as the simulated reflection coefficient gets close to zero. The average error for all three frequencies remains below 1%. When only the primary reflection coefficient mode is used, the error raises to 10% [17].

In Fig. 5, for the second simulation set, every point on the polar plot corresponds to a particular frequency and the colour of each point indicates the modelling error. A maximum error of 1.46%, 0.2% and 0.63% were observed for water, ethanol and methanol respectively. Both the experimental and simulated model validation results indicate that the model is accurate. It is worth noting that the error is particularly low in water, which suggests that the proposed model can work well in biological tissue, since it has a similar permittivity to that of water.

V. Conclusion

This paper introduced the first full-wave closed-form model for the reflection coefficient of an open-ended coaxial probe, marking a significant departure from existing modelling approaches. Previous models often face a trade-off between accuracy and simplicity. While some focus solely on the primary mode within the probe, they sacrifice accuracy by neglecting the effects of higher-order mode. Existing modelling approaches employing full wave methods involve complex and lengthy numerical manipulations that must be carried out for each measurement, resulting in a time-consuming process that is exacerbated by singularities present in numerical integrals.

Our proposed model circumvents all of these limitations at once. By presenting the forward model as simple matrix inversion, whose coefficients are independent of the MUT properties, the inverted matrix only needs to be determined once for a given probe geometry, eliminating the need for repetitive numerical integration. Our method does not only preserves the accuracy of full-wave but it also allows for efficient vectorized calculations, accelerating the solution of inverse problems where the permittivity of the tissue is extracted from the reflection coefficient. Moreover, the model may be used in real-time measurements - a crucial advancement particularly in applications such as biomedical research, where spectroscopy may provide real-time tissue identification.

In summary, the presented full-wave, closed-form model represents a harmonious fusion of accuracy and efficiency, overcoming the limitations of prior approaches. By offering both accuracy and speed, this model may pave the way for enhanced measurement capabilities in applications where precise and real-time data acquisition is crucial.

References

[1] M. Iskander et al., "A time-domain technique for measurement of the dielectric properties of biological substances," *IEEE Trans. on Instrumentation and Measurement*, vol. 21, no. 4, pp. 425–429, 1972.

[2] S. Stuchly et al., "Permittivity measurements at microwave frequencies using lumped elements," *IEEE Trans. on Instrumentation and Measurement*, vol. 23, no. 1, pp. 56–62, 1974.

[3] M. Rzepecka et al., "A lumped capacitance method for the measurement of the permittivity and conductivity in the frequency and time domain," *IEEE Trans. on Instrume. and Measur.*, vol. 24, no. 1, pp. 27–32, 1975.

[4] M. Iskander et al., "Fringing field effect in the lumped-capacitance method for permittivity measurement," *IEEE Trans. on Instrumentation and Measurement*, vol. 27, no. 1, pp. 107–109, 1978.

[5] C. McDermott, S. Lovett, and C. Rossa, "Improved bioimpedance spectroscopy tissue classification through data augmentation from generative adversarial networks," *Medical & Biological Engineering & Computing*, vol. 62, no. 4, pp. 1177–1189, 2024.

[6] C. McDermott, H. A. Bidgoli, and C. Rossa, "Observation of the ultrasonic vibration potential with an instrumented coaxial needle probe," in *2023 IEEE International Instrumentation and Measurement Technology Conference (I2MTC)*. IEEE, 2023, pp. 1–6.

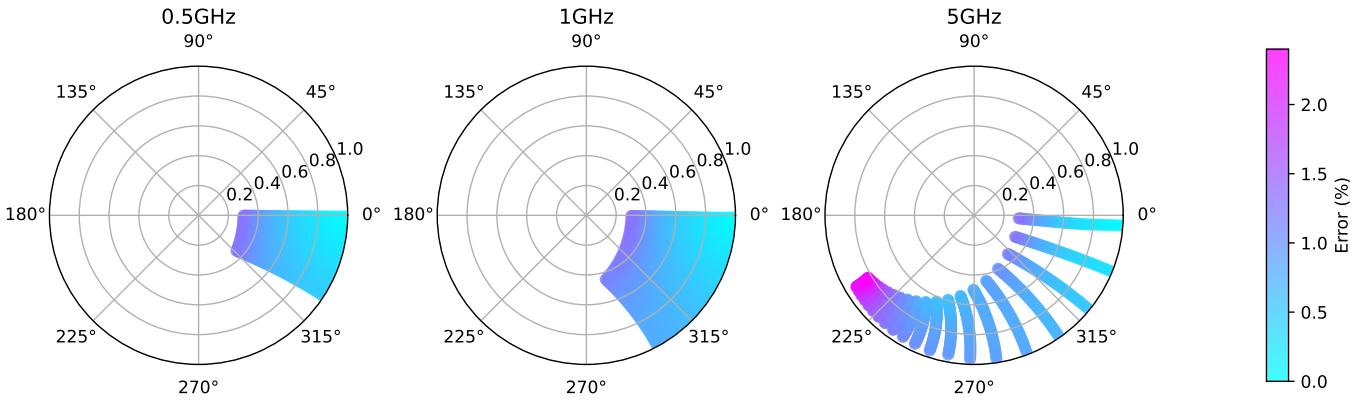

Fig. 4. Polar plots for Simulation 1. Each point on the plot corresponds to a combination of relative permittivity, which varies from $\epsilon_s = 1$ to $\epsilon_s = 100$, and conductivity, which ranges from $\sigma = 0$, S/m to $\sigma = 5$, S/m, in increments of 5 and 0.1 S/m respectively. The colour of each point indicates the error between the measured and model-predicted reflection coefficient. The frequency in each each of the three is 0.5 GHz, 1 GHz, and 5 GHz.

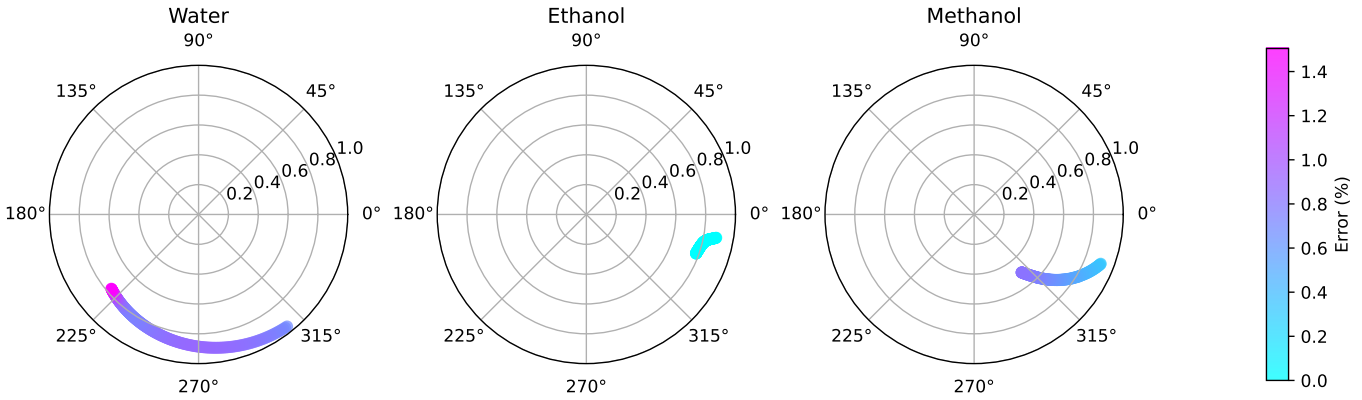

Fig. 5. Polar plots for Simulation 2. Each point on the plot represents a different frequency, ranging from 1 GHz to 5 GHz in intervals of 20 MHz. The colour of each point indicates the error between the model-predicted and simulated reflection coefficient in water, ethanol, and methanol, from left to right.

[7] M. A. Stuchly and S. S. Stuchly, "Coaxial line reflection methods for measuring dielectric properties of biological substances at radio and microwave frequencies-a review," *IEEE Trans. on Instrumentation and Measurement*, vol. 29, no. 3, pp. 176–183, 1980.

[8] I. Dilman et al., "A method to measure complex dielectric permittivity with open-ended coaxial probes," *IEEE Trans. on Instrumentation and Measurement*, vol. 71, pp. 1–7, 2022.

[9] J. Galejs, *Antennas in Inhomogeneous Media: International Series of Monographs in Electromagnetic Waves*. Elsevier, 2013, vol. 15.

[10] H. Levine and C. H. Papas, "Theory of the circular diffraction antenna," *Journal of applied physics*, vol. 22, no. 1, pp. 29–43, 1951.

[11] D. Misra et al., "Noninvasive electrical characterization of materials at microwave frequencies using an open-ended coaxial line: Test of an improved calibration technique," *IEEE Trans. on Microwave Theory and techniques*, vol. 38, no. 1, pp. 8–14, 1990.

[12] H. A. Bidgoli, N. Schieda, and C. Rossa, "Penetration depth quantification of open-ended coaxial probes for dielectric spectroscopy of layered media," in *2023 IEEE Canadian Conference on Electrical and Computer Engineering (CCECE)*. IEEE, 2023, pp. 94–98.

[13] D. Berube et al., "A comparative study of four open-ended coaxial probe models for permittivity measurements of lossy dielectric/biological materials at microwave frequencies," *IEEE Trans. on Microwave Theory and Techniques*, vol. 44, no. 10, pp. 1928–1934, 1996.

[14] A. Fallahi, S. Hashemizadeh, and N. Kuster, "On the dielectric measurement of thin layers using open-ended coaxial probes," *IEEE Transactions on Instrumentation and Measurement*, vol. 70, pp. 1–8, 2021.

[15] D. Misra, "A quasi-static analysis of open-ended coaxial lines," *IEEE Trans. on Microwave Theory and Tech.niques*, vol. 35, no. 10, pp. 925–928, 1987.

[16] S. Stuchly, C. Sibbald, and J. Anderson, "A new aperture admittance model for open-ended waveguides," *IEEE Trans. on Microwave Theory and Techniques*, vol. 42, no. 2, pp. 192–198, 1994.

[17] H. A. Bidgoli, N. Schieda, and C. Rossa, "On the sensitivity of bevelled and conical coaxial needle probes for dielectric spectroscopy," *IEEE Transactions on Instrumentation and Measurement*, 2023.

[18] D. V. Blackham and R. D. Pollard, "An improved technique for permittivity measurements using a coaxial probe," *IEEE Trans. on Instrumentation and Measurement*, vol. 46, no. 5, pp. 1093–1099, 1997.

[19] P. De anghe et al., "Design rules for an experimental setup using an open-ended coaxial probe based on theoretical modelling," *IEEE Trans. on Instrumentation and Measurement*, vol. 43, no. 6, pp. 810–817, 1994.

[20] J. Baker-Jarvis et al., "Analysis of an open-ended coaxial probe with lift-off for nondestructive testing," *IEEE Trans. on Instrumentation and Measurement*, vol. 43, no. 5, pp. 711–718, 1994.

[21] J. Mosig et al., "Reflection of an open-ended coaxial line and application to nondestructive measurement of materials," *IEEE Trans. on Instrumentation and Measurement*, no. 1, pp. 46–51, 1981.

[22] D. M. Pozar, *Microwave engineering*. John wiley & sons, 2011.

[23] P. DeLanghe et al., "Measurement of low-permittivity materials based on a spectral-domain analysis for the open-ended coaxial probe," *IEEE Trans. on Instrume. and Measurement*, vol. 42, no. 5, pp. 879–886, 1993.